Spin splitting in a *p*-type quantum well with built-in electric field and microscopic inversion asymmetry

O. Mauritz and U. Ekenberg
Theoretical Physics, Royal Institute of Technology, S-100 44 Stockholm, Sweden
(Received 14 August 1996)

The strain dependence of the spin splitting of hole subbands in modulation-doped asymmetric lattice-matched $In_xGa_{1-x}As/In_xGa_{1-x}As_yP_{1-y}$ quantum wells on lattice-mismatched $In_xGa_{1-x}As_yP_{1-y}$ substrates is investigated theoretically using a 6×6 Luttinger-Kohn Hamiltonian. The influence of the built-in electric field, the microscopic inversion asymmetry of the zinc-blende lattice, and the strain are taken into account and analyzed for different widths of the quantum wells. The spin splitting is dominated by the effects of the electric field for compressive strain and small tensile strain. For large tensile strain the microscopic inversion asymmetry is the most important origin of spin splitting. A local maximum of spin splitting is located at small tensile strain. For large compressive strain the spin splitting is strongly suppressed whereas for large tensile strain the spin splitting increases with the absolute value of strain. However, the spin splitting vanishes completely in some directions for tensile strain. [S0163-1829(97)06616-2]

I. INTRODUCTION

In two-dimensional semiconductor heterostructures the coupling between the heavy-hole and light-hole bands leads to strongly nonparabolic dispersions of the hole subbands. This is often regarded as a complication but it also gives the opportunity to modify the subbands in a controllable manner with the use of strain and doping. In particular the use of strain has been useful to improve the properties of quantum well lasers.[1,2] In quantum wells under biaxial compression the increased energy separation between the uppermost heavy-hole subband and the light-hole subbands decreases the interaction between them and decreases the parallel mass of this heavy-hole subband. This has been found to decrease the threshold current in lasers. In quantum well lasers with the active layer under sufficiently strong biaxial tension the uppermost subband is light-hole type. This gives modifications of the matrix elements for optical transitions, which are also beneficial for the properties of lasers.

It is worthwhile investigating if other properties than the parallel masses of the hole subbands can be modified by strain. In this paper we examine to what extent one can influence the subband spin splitting by strain. In a symmetric potential each hole subband has a twofold spin degeneracy. Let us denote the asymmetry due to an asymmetric potential on a scale of several lattice periods as mesoscopic asymmetry. Such an asymmetry occurs for a modulation-doped interface. A similar potential appears in a quantum well (QW) intentionally doped on one side only. In this case we have the possibility of introducing strain across a layer of finite width without causing dislocations. Spin splitting is also caused by the asymmetry on a microscopic scale in materials with zinc-blende crystal structure where the inversion symmetry is broken. We denote this kind of inversion asymmetry as microscopic asymmetry. In unstrained materials this effect is very small for III-V compounds, but a more important effect comes from the combination of inversion asymmetry and the distortion of the lattice when the material is strained. When the absolute value of strain increases, this effect will become more and more important. A study of this effect, in particular the influence of high values of strain, has been made by Silver *et al.*[3] In that paper a symmetric QW was considered. The terms due to strain-independent microscopic asymmetry were ignored since their influence is small. Especially the light-hole (LH) subbands are split and therefore these terms have the most important effect under biaxial tension.

For both cases of asymmetry the spin degeneracy is lifted for finite values of $k_\parallel$, the wave vector parallel to the interfaces. For the case of a modulation-doped interface, this has been verified experimentally.[4]

In our paper we are concerned with the situation when there is a built-in electric field over a strained $In_xGa_{1-x}As$ quantum well, which means that we also have a mesoscopic asymmetry. Zhu and Chang[5] have studied the spin splitting caused by both microscopic and mesoscopic inversion asymmetry, in particular the angular dependence of the spin splitting. They showed that the microscopic inversion asymmetry changes the symmetry of the spin splitting in the plane of the QW and that it may either increase or decrease the spin splitting. Zhu and Chang did not study the influence of deliberately strained QW's, which is the main subject of this paper.

II. METHOD

The valence-band structure is calculated self-consistently in the multiband envelope-function approximation using the Luttinger-Kohn 6×6 Hamiltonian.[6] It incorporates the heavy-hole (HH), light-hole (LH), and spin-orbit split-off (SO) band. Even if we are interested in subband energies that are small compared to the spin-orbit splitting Δ it is important to take the SO band into account because of its strain-induced coupling with the LH band. Since we deal with III-V materials we include terms due to the microscopic inversion asymmetry.[7] The strain-independent terms linear in k are normally so small that they can be safely ignored. We have verified that this can be done in our case. The Hamiltonian with strain terms but without the inversion asymmetry is[8]

 © 1997 The American Physical Society

$$H_0 = -\begin{pmatrix} \mathcal{P}+\mathcal{Q} & -\mathcal{S} & \mathcal{R} & 0 & -\frac{1}{\sqrt{2}}\mathcal{S} & \sqrt{2}\mathcal{R} \\ -\mathcal{S}^\dagger & \mathcal{P}-\mathcal{Q} & 0 & \mathcal{R} & -\sqrt{2}\mathcal{Q} & \sqrt{\frac{3}{2}}\mathcal{S} \\ \mathcal{R}^\dagger & 0 & \mathcal{P}-\mathcal{Q} & \mathcal{S} & \sqrt{\frac{3}{2}}\mathcal{S}^\dagger & \sqrt{2}\mathcal{Q} \\ 0 & \mathcal{R}^\dagger & \mathcal{S}^\dagger & \mathcal{P}+\mathcal{Q} & -\sqrt{2}\mathcal{R}^\dagger & -\frac{1}{\sqrt{2}}\mathcal{S}^\dagger \\ -\frac{1}{\sqrt{2}}\mathcal{S}^\dagger & -\sqrt{2}\mathcal{Q} & \sqrt{\frac{3}{2}}\mathcal{S} & -\sqrt{2}\mathcal{R} & \mathcal{P}+\Delta & 0 \\ \sqrt{2}\mathcal{R}^\dagger & \sqrt{\frac{3}{2}}\mathcal{S}^\dagger & \sqrt{2}\mathcal{Q} & -\frac{1}{\sqrt{2}}\mathcal{S} & 0 & \mathcal{P}+\Delta \end{pmatrix} \begin{matrix} \left|\frac{3}{2},\frac{3}{2}\right\rangle \\ \left|\frac{3}{2},\frac{1}{2}\right\rangle \\ \left|\frac{3}{2},-\frac{1}{2}\right\rangle \\ \left|\frac{3}{2},-\frac{3}{2}\right\rangle \\ \left|\frac{1}{2},\frac{1}{2}\right\rangle \\ \left|\frac{1}{2},-\frac{1}{2}\right\rangle \end{matrix} \tag{1}$$

where

$$\mathcal{P}=P_k+P_\epsilon, \quad \mathcal{Q}=Q_k+Q_\epsilon, \quad \mathcal{R}=R_k+R_\epsilon,$$

$$\mathcal{S}=S_k+S_\epsilon, \quad P_k=\left(\frac{\hbar^2}{2m_0}\right)\gamma_1(k_x^2+k_y^2+k_z^2),$$

$$Q_k=\left(\frac{\hbar^2}{2m_0}\right)\gamma_2(k_x^2+k_y^2-2k_z^2),$$

$$R_k=\left(\frac{\hbar^2}{2m_0}\right)\sqrt{3}[-\gamma_2(k_x^2-k_y^2)+2i\gamma_3 k_x k_y],$$

$$S_k=\left(\frac{\hbar^2}{2m_0}\right)2\sqrt{3}\gamma_3(k_x-ik_y)k_z,$$

$$P_\epsilon=-a_v(\epsilon_{xx}+\epsilon_{yy}+\epsilon_{zz}),$$

$$Q_\epsilon=-\frac{b}{2}(\epsilon_{xx}+\epsilon_{yy}-2\epsilon_{zz}),$$

$$R_\epsilon=\frac{\sqrt{3}}{2}b(\epsilon_{xx}-\epsilon_{yy})-id\epsilon_{xy},$$

$$S_\epsilon=-d(\epsilon_{zx}-i\epsilon_{yz}), \tag{2}$$

To the right of the matrix the values of J and M_J are given.[8] Here γ_1, γ_2, γ_3 are the Luttinger parameters, which are obtained for the alloys from linear interpolation of appropriate effective masses and are given in Table I. These input parameters including interpolation procedures for the band edges are taken from Ref. 9. Δ is the spin-orbit splitting, a_v is the hydrostatic deformation potential, and b and d the tetragonal and rhombohedral shear deformation potentials, respectively. We will only consider axial strain where

$$\epsilon_{xx}=\epsilon_{yy} \quad \text{and} \quad \epsilon_{ij}=0, \quad i\neq j,$$

which gives $R_\epsilon=S_\epsilon=0$. The effect of change in volume (P_ϵ) only shifts the band edges of the well and barriers. The difference of this shift between well and barriers is less than 2 meV and is not included. We find it convenient to use the energy shift of the HH band edge (ignoring the P_ϵ dependence) as the measure of strain: $S=Q_\epsilon=-b\epsilon_{\rm ax}$, where $\epsilon_{\rm ax}$ is the axial strain defined by $\epsilon_{\rm ax}=\epsilon_\perp-\epsilon_\parallel$. This S should not be confused with $\mathcal{S}$ in H_0.

With inversion asymmetry there are also terms proportional to k. With $\delta H_{\epsilon k}$ being the terms proportional to both strain and k, and δH_k being the terms proportional to k but not to strain, we get

$$H=H_0+\delta H_{\epsilon k}+\delta H_k, \tag{3}$$

where

$$\delta H_{\epsilon k}(\theta)=-C_4\epsilon_{ax}k_\parallel\begin{pmatrix} 0 & \frac{\sqrt{3}}{2}e^{i\theta} & 0 & 0 & \frac{\sqrt{3}}{2\sqrt{2}}e^{i\theta} & 0 \\ \frac{\sqrt{3}}{2}e^{-i\theta} & 0 & e^{i\theta} & 0 & 0 & \frac{1}{2\sqrt{2}}e^{i\theta} \\ 0 & e^{-i\theta} & 0 & \frac{\sqrt{3}}{2}e^{i\theta} & -\frac{1}{2\sqrt{2}}e^{-i\theta} & 0 \\ 0 & 0 & \frac{\sqrt{3}}{2}e^{-i\theta} & 0 & 0 & -\frac{\sqrt{3}}{2\sqrt{2}}e^{-i\theta} \\ \frac{\sqrt{3}}{2\sqrt{2}}e^{-i\theta} & 0 & -\frac{1}{2\sqrt{2}}e^{i\theta} & 0 & 0 & 0 \\ 0 & \frac{1}{2\sqrt{2}}e^{-i\theta} & 0 & -\frac{\sqrt{3}}{2\sqrt{2}}e^{i\theta} & 0 & 0 \end{pmatrix} \tag{4}$$

and

$$\delta H_k(\theta)=C\begin{pmatrix} 0 & -\frac{1}{2}e^{i\theta}k_\parallel & k_z & -\frac{\sqrt{3}}{2}e^{-i\theta}k_\parallel & 0 & 0 \\ -\frac{1}{2}e^{-i\theta}k_\parallel & 0 & \frac{\sqrt{3}}{2}e^{i\theta}k_\parallel & -k_z & 0 & 0 \\ k_z & \frac{\sqrt{3}}{2}e^{-i\theta}k_\parallel & 0 & -\frac{1}{2}e^{i\theta}k_\parallel & 0 & 0 \\ -\frac{\sqrt{3}}{2}e^{i\theta}k_\parallel & -k_z & -\frac{1}{2}e^{-i\theta}k_\parallel & 0 & 0 & 0 \\ 0 & 0 & 0 & 0 & 0 & 0 \\ 0 & 0 & 0 & 0 & 0 & 0 \end{pmatrix}. \tag{5}$$

C_4 and C are defined in Ref. 7. The values of b and C_4 are given in Table I. They were taken from Ref. 3 and since the variation is small between the materials compared to their accuracy they were taken to be the same in both well and barriers.

θ is the angle between $\mathbf{k}_\parallel=(k_x,k_y)$ and the (10) direction (the k_x direction in the k_xk_y plane). For the self-consistent calculation we use the axial approximation in which γ_2 and γ_3 in the terms R_k in Eq. (2) are replaced by $\frac{1}{2}(\gamma_2+\gamma_3)$. This influences the situation in the xy plane but the modification of the potential in the z direction due to this approximation is assumed to be small. The potential obtained by the axial approximation is used for calculations with more accurate Hamiltonians. The hole density of states is calculated numerically from the actual dispersion curves without assuming parabolicity. The temperature is 0 K in all calculations.

The subband dispersions $E(\mathbf{k}_\parallel)$ are calculated by means of a self-consistent variational method described elsewhere.[10] The spin splitting discussed below is the energy separation between two solutions at the same value of $k_\parallel$ and which are degenerate at $k_\parallel=0$. In this paper we are primarily interested in the spin splitting at moderate values of k, partly since $k_F\approx 1.5\times 10^6$ cm^{-1} when all states of the first subband with $k<k_F$ have a higher energy than the states with $k>k_F$. Another reason is that this is also the region where the spin splitting due to the mesoscopic asymmetry normally has a maximum. For definiteness we have chosen to consider the spin splitting at $k_\parallel=1.6\times 10^6$ cm^{-1}.

III. RESULTS

In this paper we have studied $In_{0.25}Ga_{0.75}As$ quantum wells with lattice-matched $In_{0.38}Ga_{0.62}As_{0.73}P_{0.27}$ barriers. The valence-band offset between these materials is 100 meV according to Ref. 9. This choice of well material permits us to achieve either tension or compression in the well because the lattice constant is intermediate between that of GaAs and InP. Mesoscopic inversion asymmetry is achieved by letting one barrier have intentional p-type doping ($N_a=3\times 10^{18}$ cm^{-3}) while the other barrier has an n-type background ($N_d=10^{15}$ cm^{-3}). The carrier concentration N_s in the well is $N_s=3\times 10^{11}$ cm^{-2} in all the cases.

Calculations have been made for six different well widths between 50 and 300 Å. By varying the composition of the barriers we could vary the strain in the quantum well but at the same time the barrier heights would change. In order to study the ''pure'' effect of strain in the quantum well we instead consider thin barriers lattice matched to the quantum well with the p-type barrier grown on a lattice-mismatched $In_xGa_{1-x}As_yP_{1-y}$ substrate with a combination of x and y such that the valence-band edge is the same in the barrier and the substrate. By varying the composition of the substrate under this condition (to avoid complications with the band bending) the lattice mismatch and hence the strain of both the quantum well and the thin barriers is tuned. The effect of the strain obtained in this way is essentially equivalent to applying external stress. The lattice mismatch and well width are kept sufficiently small that dislocations can be avoided. N_s is kept constant through all choices of materials by ad-

TABLE I. Material parameters.

	γ_1	γ_2	γ_3	b(eV)	C_4 (eV Å)
$In_{0.25}Ga_{0.75}As$	8.133	2.633	3.463	−1.72	4.71
$In_{0.38}Ga_{0.62}As_{0.73}P_{0.27}$	6.577	1.841	2.648	−1.72	4.71

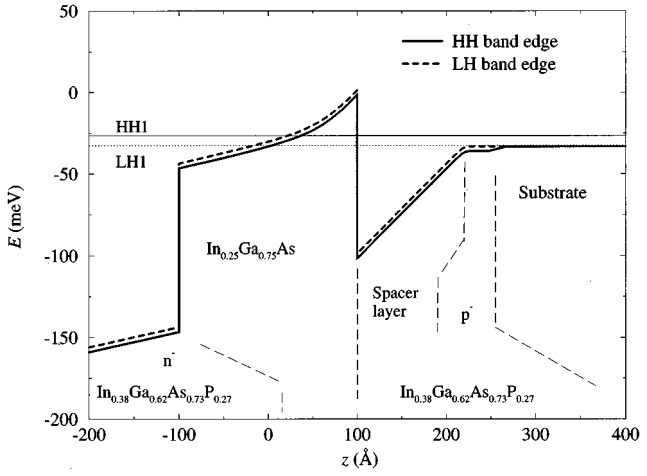

FIG. 1. Band diagram for a 200-Å $In_{0.25}Ga_{0.75}As$ quantum well between $In_{0.38}Ga_{0.62}As_{0.73}P_{0.27}$ barriers. The substrate material is $In_{0.37}Ga_{0.63}As_{0.74}P_{0.26}$, which gives a lattice mismatch of about 0.1% and $S=-2$ meV.

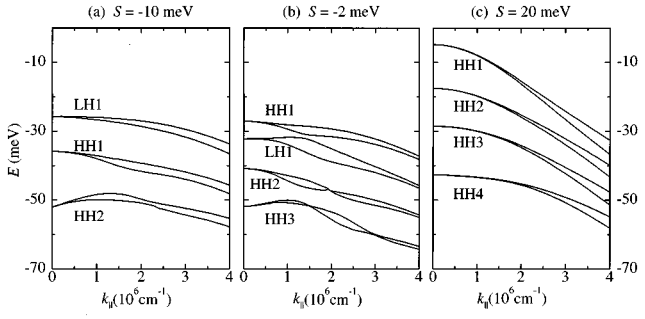

FIG. 2. Valence subband structure in the (10) direction for a 200-Å quantum well for different values of the biaxial strain. (a) is for strong tension, $S=-10$ meV, (b) for small tension, $S=-2$ meV, where the spin splitting is maximal, and (c) for strong compression, $S=20$ meV.

justing the width of the spacer layer. The width varies from 96 to 117 Å in the case of a 200-Å well. The band diagram of the 200-Å-wide well under small biaxial tension is shown in Fig. 1.

In Fig. 2 we display the subband structure for three typical cases. Using the estimated value 3.4 meV of C for GaAs (Ref. 11) the influence of δH_k is of the order of 0.1 meV. It does not depend directly on S. The influence of $\delta H_{\epsilon k}$ is a contribution to the spin splitting of the highest subband ranging from 0.0 to 1.6 meV in the (10) direction and 0.0–1.2 meV in the (11) direction in the range of S considered. It is worth noting that with inclusion of microscopic inversion asymmetry the dispersions are not the same in the (11) and $(\bar{1}1)$ directions. This is discussed further in Ref. 5.

The spin splittings for the highest subband are given for different well widths in Fig. 3. The spin splitting reaches a maximum for the wells that are between 200 and 250 Å wide whereas it is much smaller for the 50-Å- and 100-Å-wide wells. The electric field is nearly the same in all cases since it is determined by the doping. However, for the narrowest wells the left barrier confines the wave function and the difference in potential is limited in the region of the wave function and hence decreases the spin splitting. In the following we will only consider the 200-Å-wide well.

For $S<-5$ meV the highest subband is light-hole type, otherwise heavy-hole type. ($S<0$ corresponds to biaxial tension). Let us denote the highest hole subband $H1$, the next one $H2$, and so on without considering whether they are heavy-hole type or light-hole type. The results for the spin splitting for the two highest subbands are displayed in Fig. 4. Figure 2(b) shows the subband structure for small tensile strain, $S=-2$ meV, where we have maximal spin splitting. Here the spin splitting is dominated by the mesoscopic asymmetry and it is seen that the maximal spin splitting occurs near $k_{\|}\approx 1.5\times 10^6$ cm^{-1}. For large values of compressive strain [$S=20$ meV, Fig. 2(c)] the spin splitting has been reduced by a factor of 6. As long as one only considers the terms due to mesoscopic asymmetry, the spin splitting is suppressed under both tensile and compressive strain. But if $\delta H_{\epsilon k}$ is included the spin splitting is suppressed in all directions only for biaxial compression. Furthermore the effect of these linear terms is an increase of the spin splitting in the (10) direction and a decrease of it in the (11) direction. The competition between mesoscopic and microscopic asymmetry can lead to complete cancellation as seen in Fig. 4(b) for $S=-12$ meV. The spin splitting due to the microscopic asymmetry is much larger for LH subbands than for HH subbands since there are off-diagonal ϵk terms [the elements $e^{\pm i\theta}$ in the matrix (4)] that couple the different LH subbands but no corresponding terms that couple the different HH subbands. This was also shown by Ref. 3. It is seen in Fig. 2(a) that the spin splitting increases with $k_{\|}$ in contrast to Fig. 2(b).

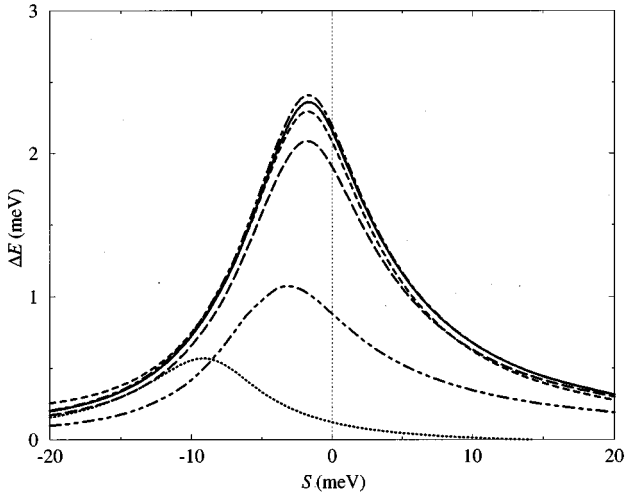

FIG. 3. Spin splitting at $k_{\|}=1.6\times 10^6$ cm^{-1} for the highest valence subband for different well widths: 50 Å (dotted line), 100 Å (double dot-dashed line), 150 Å (long-dashed line), 200 Å (solid line), 250 Å (dot-dashed line), and 300 Å (dashed line). The curves refer to the Hamiltonian H_0 in the axial approximation.

It is worth noting that the spin splittings of $H1$, $H2$, etc. are continuous even at the points where they change type, i.e., at the points where two subbands coincide at $k_{\|}=0$.[12]

When the strain is increased the heavy- and light-hole subbands become separated and their interaction is reduced. However, it is interesting to note that the subband separation is not the only factor determining the spin splittings. For example, it is seen that the maximum splitting for the two highest subbands occurs at $S\approx -2$ meV and not at $S=-5$ meV, when the energy separation of HH1 and LH1 at $k_{\|}=0$ vanishes. Interestingly enough the spin splitting is much more strongly correlated with the band mixing. In Fig. 5 the HH-LH mixture of the highest subband in the axial approximation of H_0 is shown together with the spin splitting. The mixture ξ is defined as

$$\xi=\frac{4(\|\phi_{3/2,3/2}\|^2+\|\phi_{3/2,-3/2}\|^2)(\|\phi_{3/2,1/2}\|^2+\|\phi_{3/2,-1/2}\|^2)}{\|\psi\|^2},$$

where

$$\psi(\mathbf{k}_{\|},z)=\begin{pmatrix}\phi_{3/2,3/2}(\mathbf{k}_{\|},z)\\ \phi_{3/2,1/2}(\mathbf{k}_{\|},z)\\ \phi_{3/2,-1/2}(\mathbf{k}_{\|},z)\\ \phi_{3/2,-3/2}(\mathbf{k}_{\|},z)\\ \phi_{1/2,1/2}(\mathbf{k}_{\|},z)\\ \phi_{1/2,-1/2}(\mathbf{k}_{\|},z)\end{pmatrix}$$

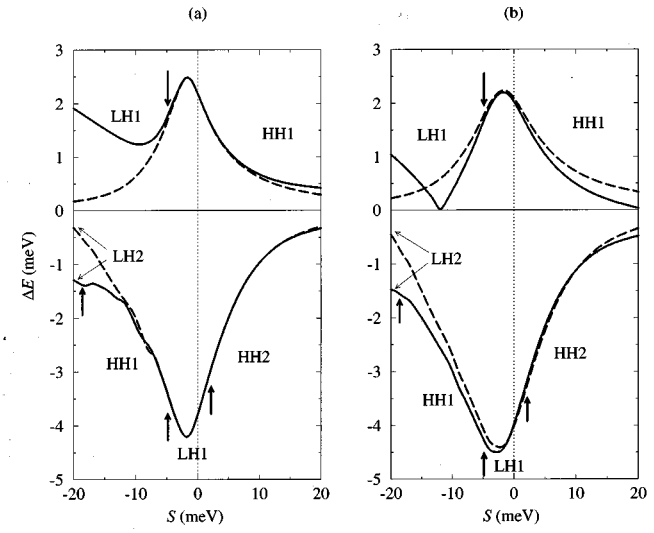

FIG. 4. Spin splitting for the highest two subbands, $H1$ (upper curves) and $H2$ (lower curves), in the (a) (10) and (b) (11) direction. The Hamiltonians are H_0 (dashed lines) and $H_0+\delta H_{\epsilon k}+\delta H_k$ (solid lines). Transitions from heavy-hole type to light-hole type of the subbands at $k_\parallel=0$ are indicated by arrows.

and ϕ_{J,M_J} denotes the envelope function corresponding to the orbital $|J,M_J\rangle$.

This definition of ξ ensures the mixture to be zero when the subband is pure HH or pure LH and reach a maximum of 1 when the subbands are half HH type and half LH type. The SO character ($\|\phi_{1/2,1/2}\|^2+\|\phi_{1/2,-1/2}\|^2$) is less than 0.015 for the QW's investigated. The role of subband mixing for the spin splitting is clear. The spin splitting due only to the mesoscopic asymmetry is almost identical in shape with the subband mixture. As pointed out in Ref. 5 this depends on the terms of the Hamiltonian, which are linear in $k_\parallel$ and which couple the different subbands. When all terms in the Hamiltonian are included the correlation between spin splitting and band mixing becomes somewhat weaker — especially for biaxial tension — since there is a linear term coupling different LH components in $\delta H_{\epsilon k}$. Still there is a strong correlation between spin splitting and band mixing.

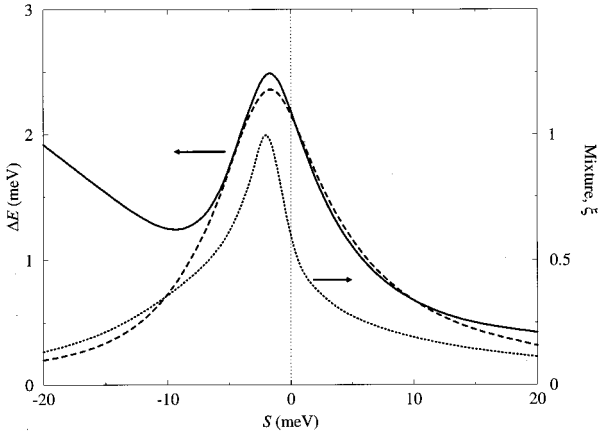

FIG. 5. Correlation between HH-LH band mixing (dotted line) and spin splitting for H_0 in the axial approximation (dashed line) and for $H_0+\delta H_{\epsilon k}+\delta H_k$ in the (10) direction (solid line).

IV. CONCLUSION

It has been shown that the spin splitting of hole subbands that occurs in asymmetric quantum wells can be strongly modified by strain. For strong compressive strain when the uppermost HH-type subband is well separated from the LH subbands the spin splitting is strongly suppressed. The spin splitting reaches a local maximum at a weak tensile strain, $S=-2$ meV. This is valid in all directions and due to the electric field induced by the modulation doping. As the tensile strain increases the spin splitting first decreases but increases again since the uppermost subband becomes LH type, which is more sensitive to the microscopic inversion asymmetry. In the (11) direction the spin splitting for the first subband vanishes at $S=-12$ meV.

ACKNOWLEDGMENT

This work was supported by the Swedish Natural Science Research Council.

[1] E. P. O'Reilly, Semicond. Sci. Technol. **4**, 121 (1989).
[2] S. W. Corzine, R.-H. Yan, and L. A. Coldren, in *Quantum Well Lasers*, edited by P. S. Zory, Jr. (Academic Press, San Diego, 1991), p. 72.
[3] M. Silver, W. Batty, A. Ghiti, and E. P. O'Reilly, Phys. Rev. B **46**, 6781 (1992).
[4] See, e.g., J. P. Eisenstein, H. L. Störmer, V. Narayanamurti, A. C. Gossard, and W. Wiegmann, Phys. Rev. Lett. **53**, 2579 (1984).
[5] B.-F. Zhu and Y. C. Chang, Phys. Rev. B **50,** 11 932 (1994).
[6] J. M. Luttinger and W. Kohn, Phys. Rev. **97**, 969 (1955).
[7] H. R. Trebin, U. Rössler, and R. Ranvaud, Phys. Rev. B **20**, 686 (1979).
[8] C. Y.-P. Chao and S. L. Chuang, Phys. Rev. B **46**, 4110 (1992).
[9] M. P. C. M. Krijn, Semicond. Sci. Technol. **6**, 27 (1991).
[10] M. Altarelli, Phys. Rev. B **28**, 842 (1983).
[11] M. Cardona, N. E. Christensen, and G. Fasol, Phys. Rev. Lett. **56**, 2831 (1986).
[12] O. Mauritz and U. Ekenberg, Surf. Sci. **361/362**, 380 (1996).